



저작자표시-비영리-변경금지 2.0 대한민국

이용자는 아래의 조건을 따르는 경우에 한하여 자유롭게

- 이 저작물을 복제, 배포, 전송, 전시, 공연 및 방송할 수 있습니다.

다음과 같은 조건을 따라야 합니다:



저작자표시. 귀하는 원저작자를 표시하여야 합니다.



비영리. 귀하는 이 저작물을 영리 목적으로 이용할 수 없습니다.



변경금지. 귀하는 이 저작물을 개작, 변형 또는 가공할 수 없습니다.

- 귀하는, 이 저작물의 재이용이나 배포의 경우, 이 저작물에 적용된 이용허락조건을 명확하게 나타내어야 합니다.
- 저작권자로부터 별도의 허가를 받으면 이러한 조건들은 적용되지 않습니다.

저작권법에 따른 이용자의 권리는 위의 내용에 의하여 영향을 받지 않습니다.

이것은 [이용허락규약\(Legal Code\)](#)을 이해하기 쉽게 요약한 것입니다.

[Disclaimer](#)

의학박사 학위논문

저온 분사 방법으로 하이드록시아파타이트
코팅한 물결 무늬 표면 PEEK 케이지의
골결합능 - 대동물 척추 유합 모델을 이용한
방사선학적, 조직형태학적, 생역학적 분석

**In vivo osseointegration property of a novel PEEK
cage with a wavy surface coated with
hydroxyapatite particles by a cold spraying
technique: A radiographic, histologic, and
biomechanical analysis with a large animal spine
fusion model**

2016년 8월

서울대학교 대학원
의학과 정형외과학 전공
김 형 민

저온 분사 방법으로 하이드록시아파타이트
코팅한 물결 무늬 표면 PEEK 케이지의
골결합능 - 대동물 척추 유합 모델을 이용한
방사선학적, 조직형태학적, 생역학적 분석

지도교수 염 진 섭

이 논문을 의학과 박사 학위논문으로 제출함

2016년 6월

서울대학교 대학원

의학과 정형외과학 전공

김 형 민

김형민의 의학박사 학위논문을 인준함

2016년 6월

위원장 구 경 회 (인)

부위원장 염 진 섭 (인)

위원 이 태 승 (인)

위원 이 준 우 (인)

위원 이 동 호 (인)

**In vivo osseointegration property of a novel PEEK
cage with a wavy surface coated with
hydroxyapatite particles by a cold spraying
technique: A radiographic, histologic, and
biomechanical analysis with a large animal spine
fusion model**

by

Hyoungmin Kim

A Thesis Submitted in Partial Fulfillment of the
Requirements for the Degree of Doctor of Philosophy
in Medicine (Orthopedics)
at the Seoul National University, College of Medicine

August 2016

Approved by thesis committee:

Professor	<u>Kyung-Hoi Koo</u>	Chairman
Professor	<u>Jin Sup Yeom</u>	Vice chairman
Professor	<u>Tae-Seung Lee</u>	
Professor	<u>Joon Woo Lee</u>	
Professor	<u>Dong-Ho Lee</u>	

Abstract

Background: A novel surface treatment for polyetheretherketone (PEEK) material, which coats it with hydroxyapatite (HA, $\text{Ca}_{10}(\text{PO}_4)_6(\text{OH})_2$) using a low temperature spraying technique, has recently been introduced to overcome the limitation of the material's bioinert property which does not allow osseointegration. The HA-coated PEEK material using the aforementioned technique has demonstrated improved osseointegration properties in a previous study following implantation in the ilium of rabbits. This study was undertaken to assess the efficacy of a novel PEEK cage coated with HA on a surface area enlarged by wavy engraving in a large animal interbody spinal fusion model.

Materials and methods: A novel cage, the surface of which was coated with HA via a cold spraying technique after the engraving of wavy lines to increase the contact area, was compared to a conventional PEEK cage with the same configurations using a large animal interbody spinal fusion model. Twelve mini-pigs underwent 4-level lumbar interbody fusion surgery via a retroperitoneal approach, with the relevant cage for implantation in each segment randomly allocated. In total, 48 empty cages (24 control and 24 experimental) were implanted without any additional graft material after disc removal and endplate

preparation. Four months after surgery, a micro-computed tomography (micro-CT) scan, histologic review, and biomechanical test under tensile stress were performed.

Results: All 12 animals were kept alive for 4 months without any significant complications after surgery: 9 segments (5 control and 4 experimental) in which the cage was dislodged or improperly placed were excluded from the analysis. The micro-CT scan and histologic analysis were performed in 35 segments (17 control and 18 experimental) and the biomechanical test was performed in 4 segments (2 control and 2 experimental). Histologic osseointegration was observed in only five segments of the experimental group and in none of the segments of the control group ($p=0.04$). The fusion rate, assessed with multi-plane-reformatted micro-CT imaging, did not differ between the groups (64.7% vs. 72.2% in the control and experimental groups, respectively; $p=0.72$). The bone volume and bone volume fraction inside and around the cage, as measured on the micro-CT scan, were not significantly different. The structural model index calculated from the micro-CT data showed an improved remodeling status for the trabecular bone in the experimental group ($p=0.032$). Biomechanical testing failed to reveal any difference between the groups.

Conclusions: Enhanced osseointegration properties of the implant surface and improved microarchitectural quality of the bridging bone

were observed in the experimental group, using a large animal interbody spinal fusion model.

Key Words: hydroxyapatite coated polyetheretherketone, spinal fusion, cold spray coating

Student Number: 2011-31117

Table of Contents

Abstract	1
Table of Contents	4
List of Tables	5
List of Figures	6
Introduction	7
Materials and Methods	11
Result	20
Discussion	27
Conclusion	31
References	32
Abstract (Korean)	35

List of Tables

Table 1. Fusion rate (micro-CT measurements)	22
Table 2. Micro-CT measurements.....	22
Table 3. The number of histologic osseointegration according to group	25
Table 4. Biomechanical test measurements.....	26

List of Figures

Figure 1. Cold spray coating	9
Figure 2. Surface (left) and cross-section (right) of polyetheretherketone (PEEK) coated with hydroxyapatite (HA) by the cold spraying technique (field scanning electron microscope [FSEM] image).	9
Figure 3. Porous HA (FSEM image)	10
Figure 4. PEEK cage with HA coating and wavy surface.....	10
Figure 5. Plain radiography of a postoperative animal.	14
Figure 6. Preparation of a specimen for micro-computed tomography (micro-CT) examination and histologic analysis.	18
Figure 7. Application of a tension force on a fused segment for biomechanical assessment.....	18
Figure 8. Micro-CT images of fusion mass and gap measurement between bone bridge.....	23
Figure 9. Histologic osseointegration (left) and no osseointegration (right)...	25
Figure 10. Stress-strain curve on tensile strength	26

Introduction

Interbody fusion surgery is one of most commonly performed procedures for the treatment of various types of degenerative spinal disorders as it restores the intervertebral disc height, spinal stability, and alignment, which are commonly impaired in spinal disorders. The procedure consists of the removal of the intervertebral disc followed by insertion of a cage, which is then filled with bone graft material of allogeneous or autogenous origin, and internal fixation of the pertinent spinal segment.

A cage made of PEEK (polyetheretherketone; $(-C_6H_4-O-C_6H_4-O-C_6H_4-CO-)_n$), a type of organic thermoplastic polymer, has been widely used because of its biomechanical advantages in load sharing and its stress distribution properties over cages constructed out of a metal, such as titanium (Kurtz et al., 2007). As the PEEK cage has an elastic modulus very similar to that of cortical bone, in comparison to titanium (Nieminen et al., 2008), it is known to result in reduced subsidence along with improved maintenance of the spinal alignment after interbody spinal fusion surgery (Kulkarni et al., 2007). However, the PEEK material has a major limitation that results from its own particular bioinert property which does not allow osseointegration, or

direct bonding, between the bone and cage (Toth et al., 2006). To overcome or circumvent this limitation, various strategies to improve the bioactivity of PEEK material were conceived including the physical or chemical treatment of its surface, and coating or impregnating it with other bioactive materials (Rui et al., 2014). PEEK material coated with hydroxyapatite (HA, $\text{Ca}_{10}(\text{PO}_4)_6(\text{OH})_2$) using a low-temperature spraying technique has recently been introduced and has showed some efficacy in osseointegration after being implanted in the ilia of rabbits (Lee et al., 2013) (Figs. 1, 2). HA, which constitutes the major part of natural bone, is reported to provide good results in osseointegration when used as a graft extender or a coating material for various implants, due to its highly osteoconductive property (Fig. 3) (Rui et al., 2014). Surface coating of the PEEK cage with HA is thought to improve its osseointegration property, while retaining its own biomechanical advantages (Lee et al., 2013). Additional wavy engraving of the implant surface will increase the surface area in contact with the surrounding bone, thus increasing the chance of osseointegration (Fig. 4). This study was undertaken to assess the efficacy of a novel PEEK cage with an HA coating in a large animal interbody spinal fusion model

Fig.1. Cold spray coating

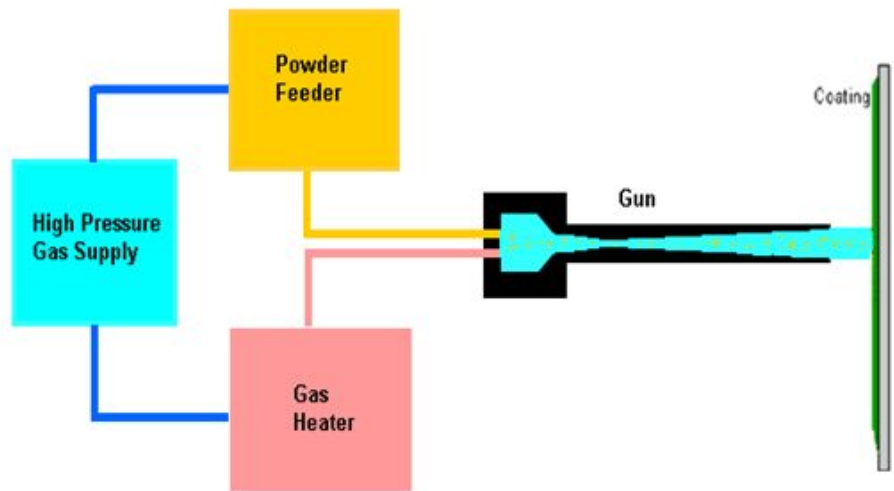


Fig.2. Surface (left) and cross-section (right) of polyetheretherketone (PEEK) coated with hydroxyapatite (HA) by the cold spraying technique (field scanning electron microscope [FSEM] image)

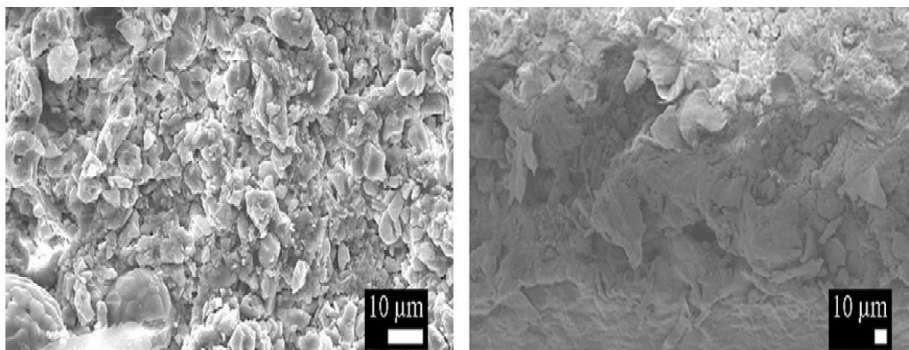


Fig.3. Porous HA (FSEM image)

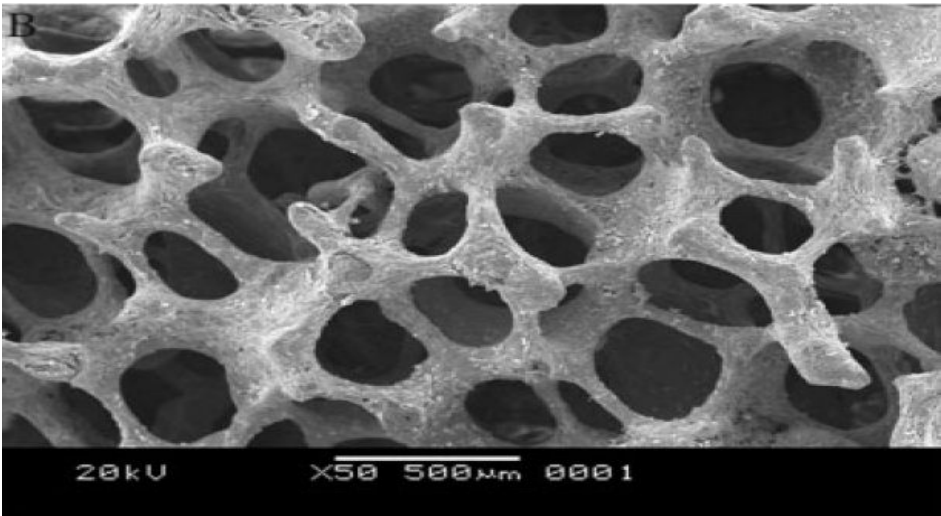
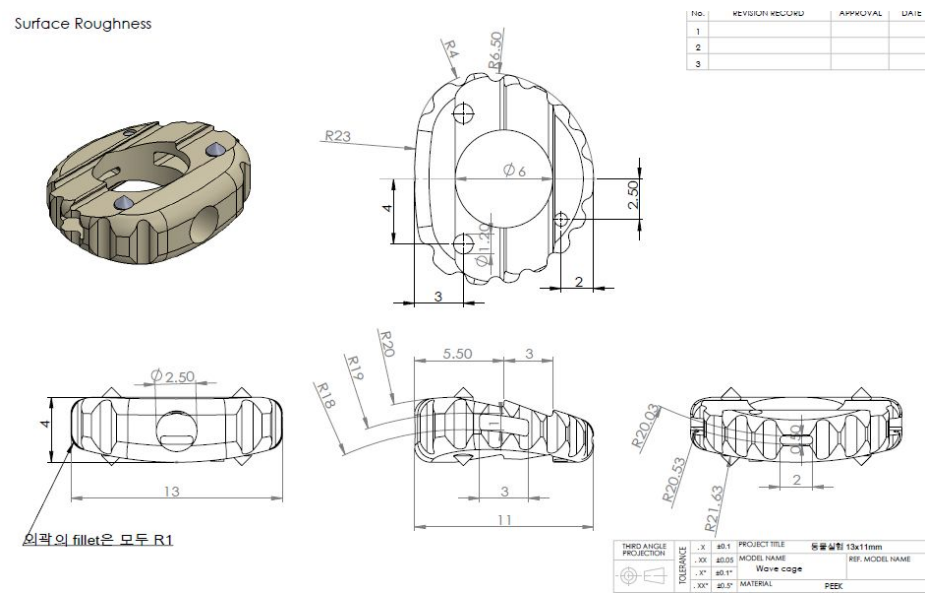


Fig. 4. PEEK cage with HA coating and wavy surface



Materials and methods

1. Animals

Twelve skeletally-matured Yucatan mini-pigs (aged 18–20 months and weighing 40–50 kg), which were obtained from the closed-barrier facility of a certified local company that provides specific pathogen-free experimental animals (Medikinetics Ltd., Pyeongtaek, Korea), were used for this study. All animals underwent 2 weeks of observation for pre-assessment and acclimatization before surgery.

2. Cages

A novel cage made of PEEK and surface-treated with wavy engraving and an HA coating applied by a low-temperature spraying technique was used for the experimental group (Fig. 4). For the control group, a conventional PEEK cage was used, which had the same configurations but lacked a surface coating of HA and wavy engraving.

3. Experimental design

Block randomization was used to decide which type of cage to implant for each level of the interbody space, maintaining a 2:2 ratio of

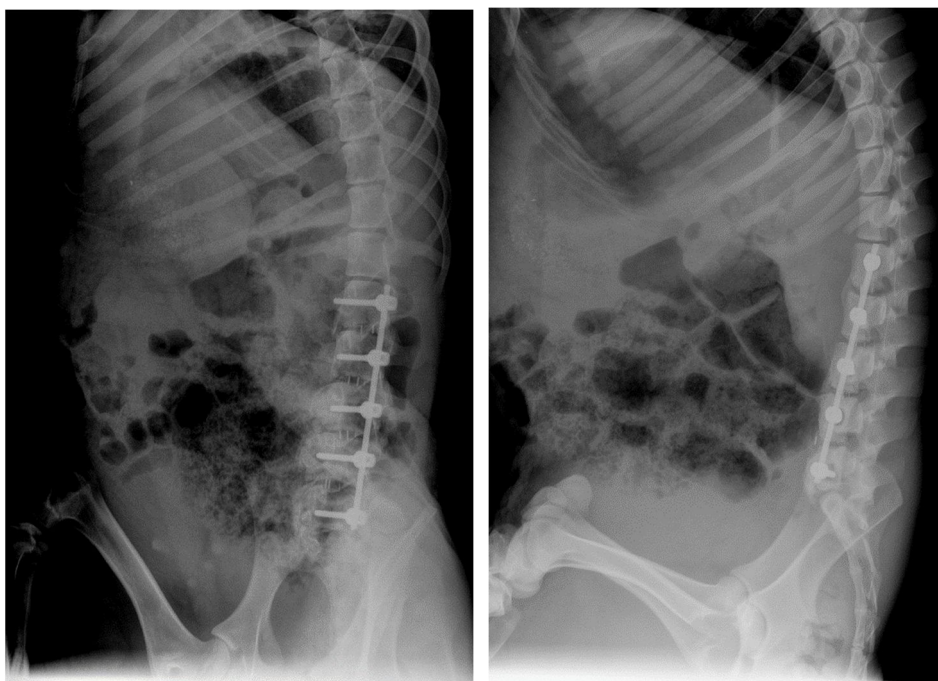
experimental and control group cages in the four levels to be fused for each animal. After surgery, the information of random allocation had been blinded until all the data was obtained. In total, 12 animals with 48 segments (24 with control cages and 24 with experimental cages) were to be used for analysis after sacrifice at 4 postoperative months. The osseointegration properties, spinal fusion, and bone formation were assessed for each segment and compared between the groups using histological specimens, micro-computed tomography (micro-CT) analysis, and biomechanical testing. The preparation of specimens, acquisition of radiologic and histologic images, and biomechanical testing were performed by blinded independent technicians. The radiologic and histologic assessment was undertaken by a single experienced spine surgeon who was also blinded of random allocation information.

4. Operative procedure

After endotracheal intubation and the induction of general anesthesia, animals were placed in the left decubitus position and prepared for operation after hair removal with an electric shaver, skin sterilization with betadine, and isolation of the operative field with draping. Anterior (or lateral) lumbar interbody fusion of four spinal segments, from L1 to L5, was performed for each animal in the following fashion.

Using a trans-retroperitoneal approach via a single oblique incision on the left flank, the lateral aspect of the lumbar vertebral column was exposed, and screws were inserted bicortically at the mid-point of each vertebral body in a direction perpendicular to the sagittal plane from L1 to L5. With the application of a distractive force to the disc space using two adjacent screws in vertebral bodies as anchors, the intervertebral disc and endplate cartilage were completely removed. After preparation of the interbody space, an empty cage (control or experimental) was implanted without any additional bone graft or graft extender for each level of the interbody space according to the previously prepared randomized order. After the insertion of four cages, a rod was connected to screw the heads together and tightened with caps via application of a compressive force for each interbody space (Fig. 5). After irrigation of the surgical field with clean saline, the wound was closed in a layer-by-layer fashion and 1 g of cephazolin was administered intravenously. Animals were sacrificed for analysis 4 months after surgery.

Fig.5. Plain radiography of a postoperative animal



5. Radiographic examinations

A. Simple radiography

Simple radiographs were taken of all animals in the anteroposterior and lateral directions at 4, 8, and 12 weeks after surgery to ensure maintenance of the surgical construct (tube-cassette distance = 60 cm; 45 kV, 2.5 mA, 12 ms).

B. 3D computed tomography (3D CT)

Prior to sacrifice, 2 of the 12 animals underwent 3D-CT 12 weeks after surgery to assess whether there was enough bone formation for analysis at the time of sacrifice.

C. Micro-computed tomography (micro-CT)

After sacrifice of the animals, the lumbar spinal columns from L1 to L5 were carefully isolated and extracted from the dead bodies. From each lumbar vertebral column, four segments were separated according to the section of the vertebral body parallel to the transverse plane at the mid-point of the L2, L3, and L4 vertebral bodies, after removal of the screws and rods, and 48 specimens – each containing segments of interest – were obtained (Fig. 6). Eight specimens were to be preserved for biomechanical testing and a further forty specimens were to be

examined with high-resolution micro-CT (SkyScan 1173; Skyscan N.V., Kontich, Belgium) using an aluminum 1.0 mm filter with a source voltage of 130 kV and source current of 30 μ A. The image pixel size was 19.89 μ m and the rotation angle of the specimens was 0.4°. Using image-reformatting software (Dataviewer; Skyscan N.V.) and image-analyzing software (CTAn; Skyscan N.V.), spinal fusion or bony union, and the quality and quantity of bone formation inside and around the cage, were assessed for each segment and compared between the groups. Bony union or spinal fusion was defined by the presence of continuity or a less-than-1-mm gap in the trabeculae bridging, which can be observed in the reformatted images of the coronal or sagittal plane inside or around the cage between adjacent vertebral bodies. For the quantitative analysis of new bone formation and maturation inside the cage, the trabecular bone microarchitecture in the volume of interest (VOI; 3D region of interest) was measured in each specimen and the following variables were calculated for analysis: tissue volume (TV), bone volume (BV), bone volume fraction (BV/TV), trabecular thickness, trabecular number, trabecular separation, bone surface/volume ratio, and structural model index (SMI) (Hildebrand et al., 1997).

6. Histologic analysis

After micro-CT examination, 40 specimens were fixed for 24 hours in a 10% neutral buffered formalin solution, sequentially dehydrated in alcohol and cleaned in xylene, and then embedded in a graded catalyzed methyl methacrylate. After polymerization, the specimens were trimmed and sectioned using a diamond cutter (Exakt300cp; Exakt Co., Norderstedt, Germany). At least 10 40- to 50- μ m-thick sections around the mid-sagittal plane were produced. Undecalcified sections were stained with hematoxylin and eosin and reviewed.

Histologic osseointegration was assessed following Branemark's definition of implant osseointegration; that is, direct contact between the living bone and implant should be observed under light microscopy in between the bone-implant interface with a lack of non-bony tissue interposition as a result of a negative tissue response, such as inflammation (Branemark, 1983).

Fig. 6. Preparation of a specimen for micro-computed tomography (micro-CT) examination and histologic analysis. Spinal column (left upper), the cutting of each segment (left lower), mid-sagittal cut surface of the segment (right).

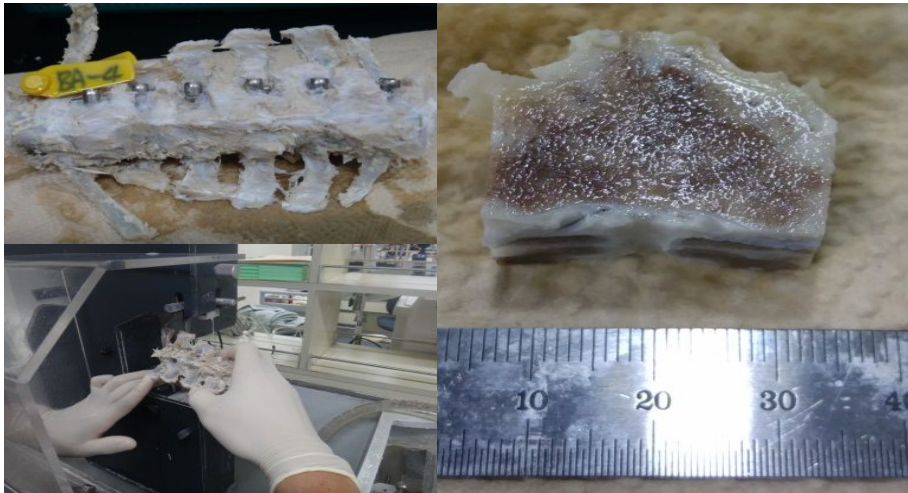


Fig. 7. Application of tension force on fused segment for biomechanical assessment



7. Biomechanical test

Biomechanical testing was performed for eight specimens (four control and four experimental) to measure the stress and strain curve using an Instron testing machine (DTU-900 MH (200 kN); Daekyung Tech Co., Incheon, Korea) which applied tensile strength under the conditions of a calibrated load-cell of 10 N and a crosshead speed range of 5 mm/min.

8. Statistical analysis

Statistical analysis was performed with SPSS for Windows software (ver. 18.0; SPSS Inc., Chicago, IL, USA). Fisher's exact test or the chi-squared test were used to compare qualitative variables, such as the fusion status, between groups. Student's t-test was used for quantitative continuous variables such as the parameters of the micro-CT analysis. A *P*-value less than 0.05 was considered to have statistical significance.

Results

1. Animals and specimen

All 12 animals survived for 4 months after 4-level anterior lumbar interbody fusion surgery, without any complications that could have affected the results of the study. From the lumbar vertebral column of the 12 animals, 48 specimens were obtained for analysis.

2. Simple radiography

Sequential simple radiographs, taken on three occasions during the 4-week interval after surgery, revealed four segments with improper placement or dislodgement of the cage. These were excluded from further analysis with micro-CT, histology sectioning, or biomechanical study.

3. 3D-CT

Two animals selected at random underwent a 3D-CT scan at 12 postoperative weeks. Abundant bone formation for analysis was observed and all animals were sacrificed as planned at 16 postoperative weeks.

4. Micro-CT

Micro-CT scanning was performed for 35 specimens, except for 4 specimens (2 control and 2 experimental) that were randomly selected and reserved for (destructive) biomechanical testing, and a further 9 segments (5 control and 4 experimental) that were displaced out of the interbody space. The fusion rate, assessed with multi-plane-reformatted micro-CT imaging, did not differ between the groups: 64.7% vs. 72.2% in the control and experimental groups, respectively ($p=0.72$) (Table 1). The VOI for quantitative assessment with micro-CT was confined to the inside of the cage to minimize the effect of any difference in cage location within the disc space. The measured BV was not found to be different between the groups: $21.8 \pm 14.4 \text{ mm}^3$ and $18.6 \pm 11.9 \text{ mm}^3$ in the control and experimental groups, respectively ($p=0.475$). The calculated BV/TV, trabecular thickness, trabecular number, trabecular separation, and bone surface/volume ratio showed no significant difference. However, the SMI was found to be significantly closer to 0 in the experimental group (Table 2, Fig. 8).

Table 1. Fusion rate (micro-CT measurements)

	Group (N=35)		<i>P</i> -value*
	Control	Experimental	
Non-fusion	6	5	0.724
Fusion	11	13	
Fusion rate	64.7%	72.2%	

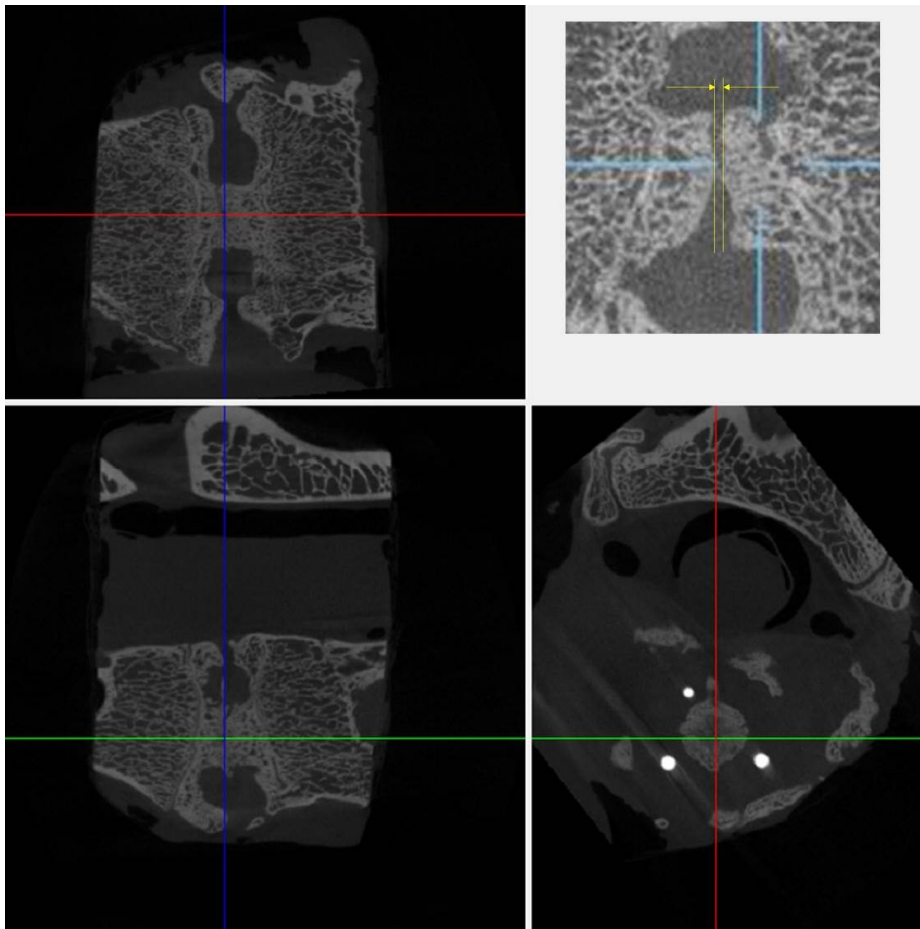
**P* value by Fisher's exact test

Table 2. Micro-CT measurements

	Group (N=35)		<i>P</i> -value
	Control (n=17)	Experimental (n=18)	
Bone bridge gap distance (mm)	1.26±1.88	1.01±1.88	0.693
Bone volume (mm ³)	21.89±14.48	18.65±11.99	0.475
Tissue volume (mm ³)	112.23±0.32	112.02±3.56	0.179
Bone volume fraction (%)	19.51±11.99	16.63±10.67	0.476
Bone surface (mm ²)	339.36±166.01	326.35±173.45	0.822
Bone surface volume ratio	17.29±4.10	18.98±3.24	0.184
Structural model index*	-2.26±1.98	-0.91±1.54	0.032*
Trabecular thickness	0.17±0.02	0.17±0.03	0.174
Trabecular number	1.10±0.61	0.98±0.59	0.556
Trabecular separation	1.62±0.63	1.64±0.56	0.906

*Values show a statistically significant difference between the groups according to Student's *t*-test

Fig. 8. Micro-CT images of fusion mass and gap measurement between bone bridge



5. Histologic analysis

Histologic osseointegration was observed in five specimens of the experimental group only (Fig. 9). The ratio of histologic osseointegration was significantly higher in the experimental group ($p=0.04$) (Table 3).

Fig. 9. Histologic osseointegration (left) and no osseointegration (right) ($\times 40$ light microscope with hematoxylin and eosin staining, following non-decalcified preparation).

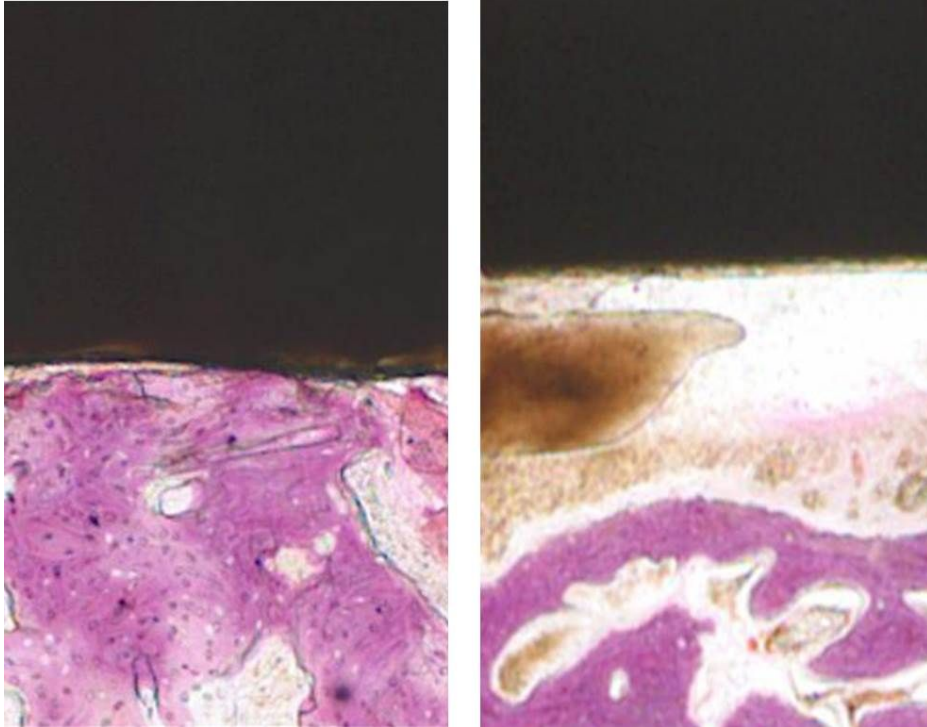


Table 3. The number of histologic osseointegration according to group

	Group (N=35)		<i>P</i> -value*
	Control (n=17)	Experimental (n=18)	
Osseointegration	0	5	0.04
No osseointegration	17	13	

*Values show a statistically significant difference between groups according to Fisher's exact test

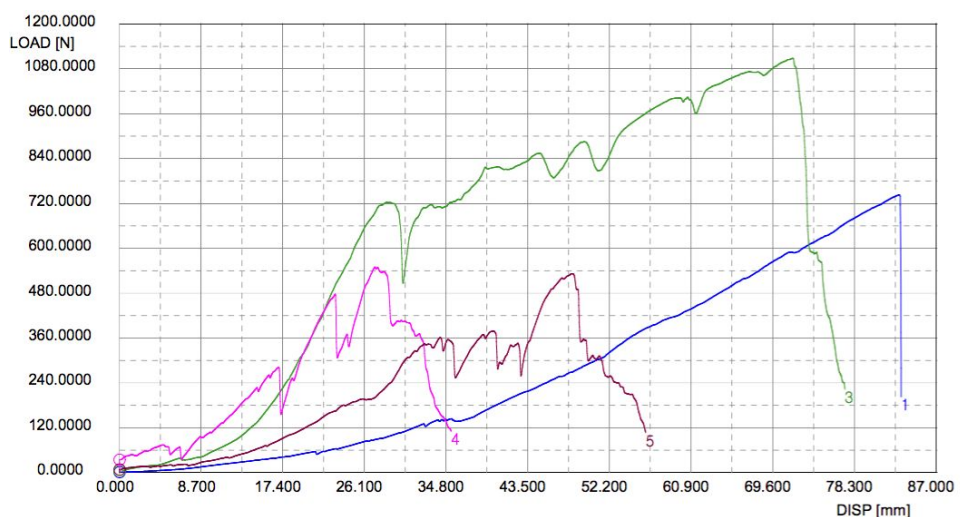
6. Biomechanical test

Tensile strength and load, and yield strength and load, were measured for the four fused segments: two with the conventional PEEK cage and two with the experimental PEEK cage. The results are shown in Table 4 and Fig. 10, and there was no significant difference between the groups ($p=0.572$).

Table 4. Biomechanical test measurements

	Specimen (n=4)			
	Control 3	Control 5	Experimental 1	Experimental 4
Maximal load (N)	1106.40	531.60	741.80	549.00
Tensile strength (N/mm ²)	1106.40	531.60	741.80	549.00
Yield strength (N)	4.20	8.60	1.40	34.40
Yield load (N/mm ²)	4.20	8.60	1.40	34.40

Fig. 10. Stress-strain curve on tensile strength



Discussion

Branemark demonstrated that titanium implants could become permanently incorporated within living bone, i.e. that histologic observation had revealed direct bone-to-implant contact without the interposition of non-osseous tissue (osseointegration or osteointegration; Branemark, 1959). Following his concept of osseointegration, "a direct structural and functional connection between ordered, living bone and the surface of a load-carrying implant" (Branemark, 1983), modern dental and orthopedic endoprostheses have since been developed.

Within this study, which used a novel PEEK cage coated with HA by a cold spraying technique in a large animal lumbar interbody fusion model, direct bone contact without interposition of non-osseous tissue was observed histologically in only the experimental group (5 out of 18 specimens). Although the rate of osseointegration was less than 30%, there was a significant difference between the groups since no such osseointegration was found in the control group.

Osseointegration is known to follow the bone healing process around implants, involving a cascade of cellular and extracellular biological events at the bone-implant interface until the implant surface appears to be finally covered with newly-formed bone (Mavrogenis et al., 2009).

The smooth, hydrophobic, and bioinert surface of the bare PEEK material limits cellular and protein attachment. Treatment of the PEEK surface with an HA coating changes its surface to a rough, hydrophilic, and biocompatible one, which is beneficial for cellular adhesion and viability (Rui et al., 2014).

Lee et al. previously reported the in vitro and in vivo testing of HA-coated PEEK by the same cold spraying technique, and their results showed improved adhesion, viability, and osteoblast differentiation of human bone marrow mesenchymal stem cells on the surface of HA-coated PEEK compared with bare PEEK (Lee et al., 2013). They also demonstrated that HA-coated PEEK promoted osseointegration and the formation of new bone around the implant using a rabbit ilium model with histomorphometry and micro-CT analysis.

The discrepancy in the results pertain to the osseointegration rate, between the current study and the previously performed study that used a rabbit iliac crest model, derives from differences in the mechanical stress loading and micro-motion of the implant. An oscillating displacement of the implant within 20 μm is known to allow osseointegration, whereas motion exceeding 40–150 μm compromises or inhibits it (Bragdon et al., 1996). The instrumentation used in the current experiment is not thought to provide enough fixation power to control the physiologic segmental motion of the lumbar spine (to

provide a higher osseointegration rate). Experimental design using empty cage implantation without any additional bone graft is also thought to work against osseointegration, although it might help to emphasize the difference in bone formation quality. Another limitation to consider in the interpretation of the histologic results is the destructive nature of specimen preparation; such procedures do not guarantee the preservation of integrity in bone contact with the implant surface or osseointegration achieved in vivo.

The results of the micro-CT analysis performed in this study did not reveal any quantitative difference in bone formation inside and around the cage. The quantity of bone formation measured by micro-CT as a parameter of the BV and BT/TV ratio did not differ. The fusion rate was approximately 64% in the control group and about 72% in the experimental group, but this difference was not significant. The average BV/TV measured inside the cage was around 20% in both groups, which is close to the value of the reported BV/TV of human lumbar vertebrae (Acquaah et al., 2015), reflecting the successful induction of the physiological bone healing process in this experiment even though no additional bone graft material was applied.

However, the SMI, an index of trabecular maturation in the microarchitecture, was significantly different between the groups. The SMI indicates the relative prevalence of rods and plates in a 3D

structure such as the trabecular bone (Hildebrand et al., 1997). An ideal plate, cylinder, and sphere have SMI values of 0, 3, and 4, respectively. Conversely, cylindrical and spherical cavities have SMIs of -3 and -4, respectively (morphometric parameters measured by the Skyscan™ CT analyzer software). The plate-like trabecular bone is known to be associated with greater mechanical strength than the rod-like trabecular bone. Trabecular bone is also known to transit from plate-like to rod-like architecture in osteoporotic degradation. Recently, the microarchitecture of bone is increasingly being considered as an adjuvant or viable alternative to bone density for the evaluation of the bone status.

That the SMI result was much closer to 0 in the experimental group can be interpreted as indicating that the new bone formed inside the experimental cage was more mature than that inside the control cage. This is thought to reflect one of the potential benefits of the HA coating. Since the coating might affect trabecular bone formation, i.e., woven bone formation through the facilitation of marrow connections and biologic fixation, and this new bone is eventually remodeled into lamellar bone that is in direct contact with most of the implant surface (osseointegration) (Mavrogenis et al., 2009), a larger mineral surface area afforded by the complex trabecular network can provide a vast substrate on which directed cellular activity can interact with the bone

mineral material (Burr, 2002).

Interpretation of the results of the biomechanical test, which failed to identify a superior group, should be deferred considering the insufficient number of specimens used in this study.

Conclusion

The fusion rate was slightly higher in the experimental group without any statistical significance. The osseointegration was observed only in the experimental group (in 5 of 18 specimens). The results of this study could have been improved with more rigid fixation and application of additional bone graft material, particularly in terms of the assessment of direct osseointegration. Using a mini-pig lumbar interbody fusion model, the current study showed some potential benefit and confirmed non-inferiority of the novel PEEK cage with a cold spray coating of HA in comparison to the conventional PEEK cage. Further study is required to find any practical benefit in a clinical setting.

References

Acquaah F, Robson Brown KA, Ahmed F, Jeffery N, Abel RL. Early Trabecular Development in Human Vertebrae: Overproduction, Constructive Regression, and Refinement. *Frontiers in Endocrinology*. 2015;6:67.

Bragdon CR, Burke D, Lowenstein JD, O'Connor DO, Ramamurti B, Jasty M, Harris WH. Differences in stiffness of the interface between a cementless porous implant and cancellous bone in vivo in dogs due to varying amounts of implant motion. *J Arthroplasty* 1996;11:945-51.

Brånemark PI. Vital microscopy of bone marrow in rabbit. *Scand J Clin Lab Invest* 1959;11(Suppl.38):1-82.

Brånemark PI. Osseointegration and its experimental studies. *J Prosthet Dent* 1983;50:399-410.

Burr DB. Targeted and non-targeted remodeling. *Bone* 2002;30, 2–4

Hahn M, Vogel M, Pompesius-Kempa M, Delling G. Trabecular bone pattern factor--a new parameter for simple quantification of bone microarchitecture. *Bone*. 1992;13(4):327-30.

Hilderand T, Rüdsegger P. Quantification of Bone Microarchitecture with the Structural Model Index. *Comp Meth Biomech Biomed Engin*,

1997;1(1):15-23.

Hildebrand T, Laib A, Müller R, Dequeker J, Rügsegger P. Direct three-dimensional morphometric analysis of human cancellous bone: microstructural data from spine, femur, iliac crest, and calcaneus. *J Bone Miner Res.* 1999;14(7):1167–1174.

Kulkarni AG, Hee HT, Wong HK. Solis cage (PEEK) for anterior cervical fusion: preliminary radiological results with emphasis on fusion and subsidence. *Spine J.* 2007;7(2):205e9.

Kurtz SM, Devine JN. PEEK biomaterials in trauma, orthopedic, and spinal implants. *Biomaterials.* 2007;28(32):4845e69.

Lee JH, Jang HL, Lee KM, Baek HR, Jin K, Hong KS, Noh JH, Lee HK. In vitro and in vivo evaluation of the bioactivity of hydroxyapatite-coated polyetheretherketone biocomposites created by cold spray technology. *Acta Biomater.* 2013 Apr;9(4):6177-87.

Mavrogenis AF, Dimitriou R, Parvizi J, Babis GC. Biology of implant osseointegration. *J Musculoskelet Neuronal Interact.* 2009; 9(2):61-71.

Mittra E, Rubin C, Qin YX. Interrelationship of trabecular mechanical and microstructural properties in sheep trabecular bone. *J Biomech.* 2005 Jun;38(6):1229-37.

Nieminen T, Kallela I, Wuolijoki E, Kainulainen H, Hiidenheimo I, Rantala I. Amorphous and crystalline polyetheretherketone:

mechanical properties and tissue reactions during a 3-year follow-up. *J Biomed Mater Res A*. 2008;84A:377–83.

Rui Ma, Tingting Tang. Current Strategies to Improve the Bioactivity of PEEK. *Int J Mol Sci*. 2014;15:5426-45.

Toth JM, Wang M, Estes BT, Scifert JL, Seim III HB, Turner AS. Polyetheretherketone as a biomaterial for spinal applications. *Biomaterials*. 2006;27(3):324e34.

국문 초록

목 적: 저온 분사 방법을 이용해 표면을 수산화인회석 (hydroxyapatite) 으로 코팅하고 물결 무늬 처리한 polyetheretherketone (PEEK) 소재 케이지 (cage) 의 추체간 척추유합술에서의 유용성을 척추가 인간과 유사한 대동물인 mini-pig 를 이용하여 평가하였다.

대상 및 방법: mini-pig 12 마리를 대상으로 4 분절 추체간 유합술을 후복막강 경유 전방접근법으로 시행하였다. 전신 마취 하에 수술을 시행하였으며, 블록무작위 배정을 통하여 각 실험 동물 개체 내 실험군과 대조군 임플란트 (implant)를 삽입할 분절을 결정하였다. 실험군 임플란트로는 저온 분사 방법을 이용해 표면을 수산화인회석 (hydroxyapatite)로 코팅하고 물결 무늬 처리한 polyetheretherketone (PEEK) 소재로 만든 새로운 케이지 (cage) 를 사용하였고 대조군으로는 PEEK 단일 소재로 만든 채래식 임플란트를 사용하였다. 수술 후 4 주, 8 주, 12 주에 전후방 및 측방 단순 방사선 검사를 촬영하고, 4 개월간 생육한 후 희생하여, 8 분절 (실험군 대조군 각 4 분절씩) 에 대해서는 생역학적 평가를 위해 인장 시험을 시행하고 나머지 40 분절에 대하여서는 미세 전산화 단층 촬영(micro-CT) 및 조직학적 검사를 시행하여 골결합, 유합 여부, 골조직 생성 정도를 판정하였다.

결 과: 동물 실험 결과 12 마리의 개체 모두 생육 기간 동안 생존하였으며 생역학적 검사를 위한 4 분절(실험군과 대조군 각각 2 분절), 단순 방사선 검사 소견상 임플란트 이탈 (대조군 5 분절, 실험군 4 분절) 로 분석의 가치가 없어 보이는 9 분절을 제외한, 총

35 분절에서 조직학적 검사 및 미세전산화 단층 촬영 분석을 시행하였다. 골결합 (osseointegration) 은 실험군에서만 관찰되었으며 18 분절중 5 개 분절에서 확인되었다. 미세 전산화 단층 촬영 검사에서 확인한 유합은 대조군 케이지를 사용한 분절 17 개 중 11 개(64.7%), 실험군 케이지를 사용한 18 분절 중 13 개(72.2%)이었으며 이는 통계적으로 유의한 차이를 보이지 않았다($P=0.724$). 여기서 측정한 케이지 내부의 골부피(bone volume, BV), 골부피 비율(bone volume fraction, bone volume/tissue volume), 골소주의 두께, 숫자 및 분리 정도(trabecular thickness, number, separation)에서도 통계적으로 유의한 군간의 차이는 없었다. 하지만 구조적 모델 지수 (structural model index, SMI) 는 통계적으로 유의한 차이를 보였으며 실험군에서 0 에 가까운 값을 보였다.

실험 동물의 생육 기간 중 실험 결과에 영향을 미칠만한 합병증은 발생하지 않았다. 생역학적 분석 결과에서는 검체 수 부족으로 통계적으로 유의한 차이를 얻지 못했다.

결 론: 대동물 추체간 유합 실험 결과 골이식재의 추가적인 적용 없이 PEEK 케이지 만으로도 일정 비율에서 추체간 유합을 얻을 수 있으며, 표면을 생체활성 HA 코팅하고 물결무늬 굴곡 구조를 적용할 경우 골결합 (osseointegration) 에 유리하고 보다 정교한 해면골 구조를 유도할 수 있는 가능성을 확인하였다.

색인 단어: 수산화인회석 (hydroxyapatite, HA), 추체간 유합술, PEEK

학 번: 2011-31117